Coupled-channels Calculations of Heavy-ion Fusion Reactions

Henning Esbensen

Argonne National Laboratory, Argonne, Illinois, USA

- The goal is to develop a coupled-channels description that can explain phenomena observed in heavy-ion fusion reactions, e.g,
  a) large enhancement at energies below the CB (Coulomb barrier),
  b) hindrance of fusion at extreme sub-barrier energies,
  c) suppression of fusion data far above the CB.
- The description should include couplings to
  a) low-lying 2^+ and 3^- states, mutual and two-phonon exc.,
  b) excitations of rotational states (if deformed),
  c) transfer channels: 1n, 2n, 1p, 2p, α (if necessary.)

Work supported by U.S. Department of Energy,
Office of Nuclear Physics

Argonne NATIONAL LABORATORY

- Such couplings usually explain the enhancement below the CB.

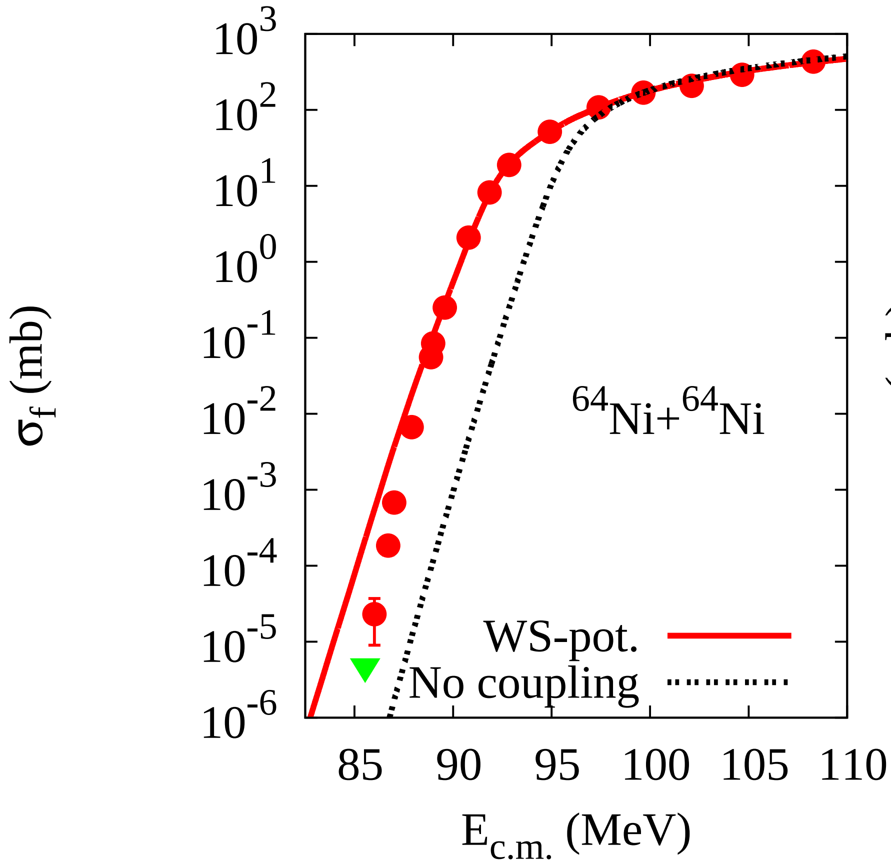

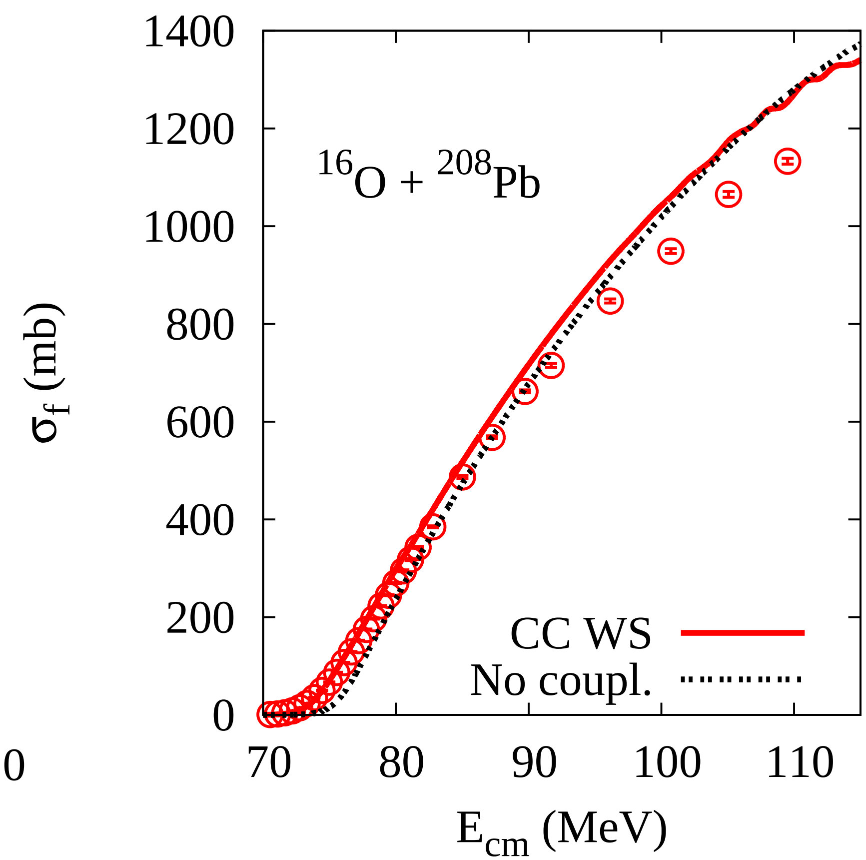

^{64}Ni+^{64}Ni by Jiang et al., PRL 93, 012701 (2004).

^{16}O+^{208}Pb by Morton et al., Phys. Rev. C 60, 044608 (1999).

- In the 1970s fusion cross sections were measured at energies above the Coulomb barrier. Once you overcome a barrier you are trapped.
- Since the 1980s cross sections down to 0.1 mb were measured. Large enhancements observed. Coupled-channels calculations were developed. Once you have penetrated the barrier you are trapped.
- Since 2001 cross sections have been measured down to 10 nb. Large hindrance compared to coupled-channels calculations. Calculations are sensitive to the ion-ion potential in the interior.
- Coupled-channels calculations must be based on a realistic ion-ion potential, with a realistic pocket above the Compound Nucleus GS.
- The calculations should explain the hindrance far below the CB, and help explain the suppression far above the CB.
- EXAMPLES: ^{64}Ni+^{64}Ni, ^{16}O+^{208}Pb, ^{16}O+^{16}O.

Proximity type Woods-Saxon (WS) potential

$$U(r) = \frac{-16\pi\gamma a R_{aA}}{1+\exp[(r-R_a-R_A)/a]},$$

where γ is the nuclear surface tension and $a \approx$ 0.6 - 0.7 fm.

It is realistic for large values of r, where it is consistent with elastic scattering data (Rex-Winther) and with double-folding potentials (Akyüs-Winther). It provides a good description of the height of the Coulomb barrier and of fusion data with $\sigma_f \geq 0.1$ mb.

The force has the correct liquid drop form for touching spheres:

$$F = -4\pi\gamma R_{aA}, \quad \text{where} \quad R_{aA} = \frac{R_a R_A}{R_a + R_A}.$$

This type of potential has been very useful in the past.
However, it is not realistic for overlapping nuclei.

Coupled-channels formalism.

Expand total wave function on channel-spin wave functions,

$$\Psi_{JM} = \sum_{nIL} \frac{\psi_{nIL}(r)}{r} \, |n(IL)JM\rangle.$$

Channel-spin wave functions

$$|n(IL)JM\rangle = \sum_{M_L M_I} \langle LM_L, IM_I|JM\rangle \, |LM_L\rangle \, |nIM_I\rangle.$$

$|L, M_L\rangle$ orbital angular momentum,

$|nIM_I\rangle$ excited state of projectile or target,

$|J, M\rangle$ total spin, which is conserved.

Coupled equations: $(h_L + \epsilon_{nI} - E)\, \psi_{nIL}(r) =$

$$- \sum_{n'I'L'} \langle n(IL)JM|V_{int}|n'(I'L')JM\rangle \, \psi_{n'I'L'}(r).$$

$I + 1$ channels for each state: $L' = |L - I|$, ... ,$L + I|$. TOO MANY!

Rotating frame approximation.

- Assumes that the orbital angular momentum L is conserved (also known as the Iso-centrifugal approximation.)
- Then one can diagonalized the interaction matrix in such a way that there is only one channel for each excited state (nI) instead of $I+1$ channels, namely, the state $|nIM>$, where M is conserved.
- For fixed L solve the coupled equations:

$$(h_L + \epsilon_{nI} - E)\,\psi_{nI}(r) = -\sum_{n'I'} \langle nI|V_{int}|n'I'\rangle\,\psi_{n'I'}(r).$$

Good approximation for fusion; not so good for angular distributions of Coulomb excitation and transfer reactions at forward angles.

Example: Quadrupole excitations.

- Consider quadrupole excitations.
- The full problem has $\sum(I+1)$ = 33 channels.
- In the rotating frame approximation, there is only one channel (M=0) for each state, i. e., we only need $\sum 1$ = 10 channels.

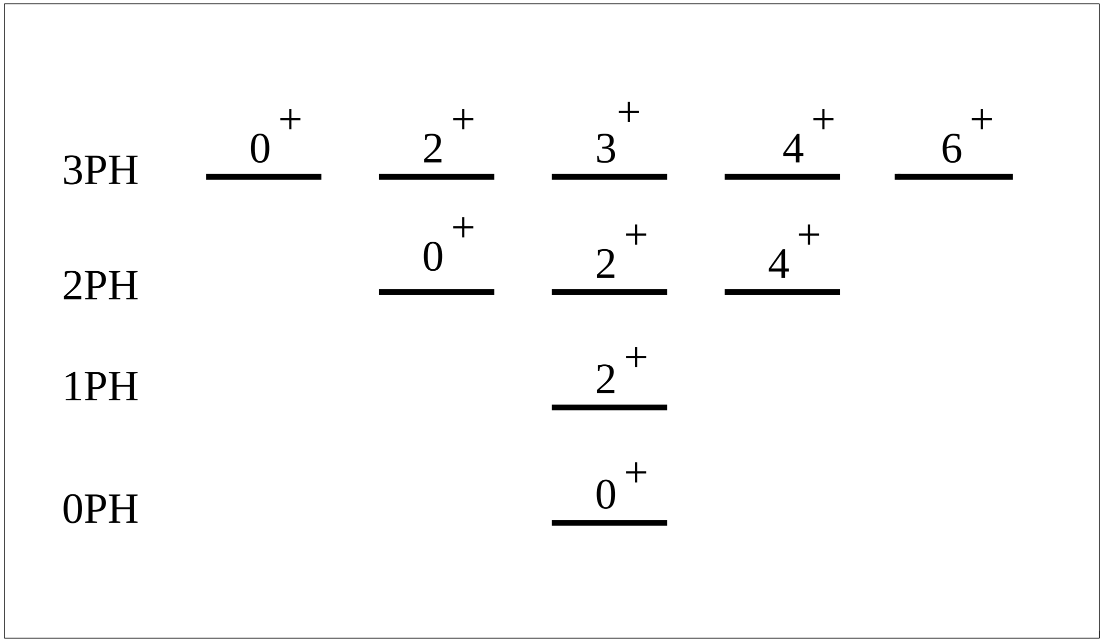

- Combine the (3) two-phonon and the (5) three-phonon states into one effective two-phonon and three-phonon state, respectively. Only 4 effective channels are needed.

Standard two-phonon calculation of fusion.

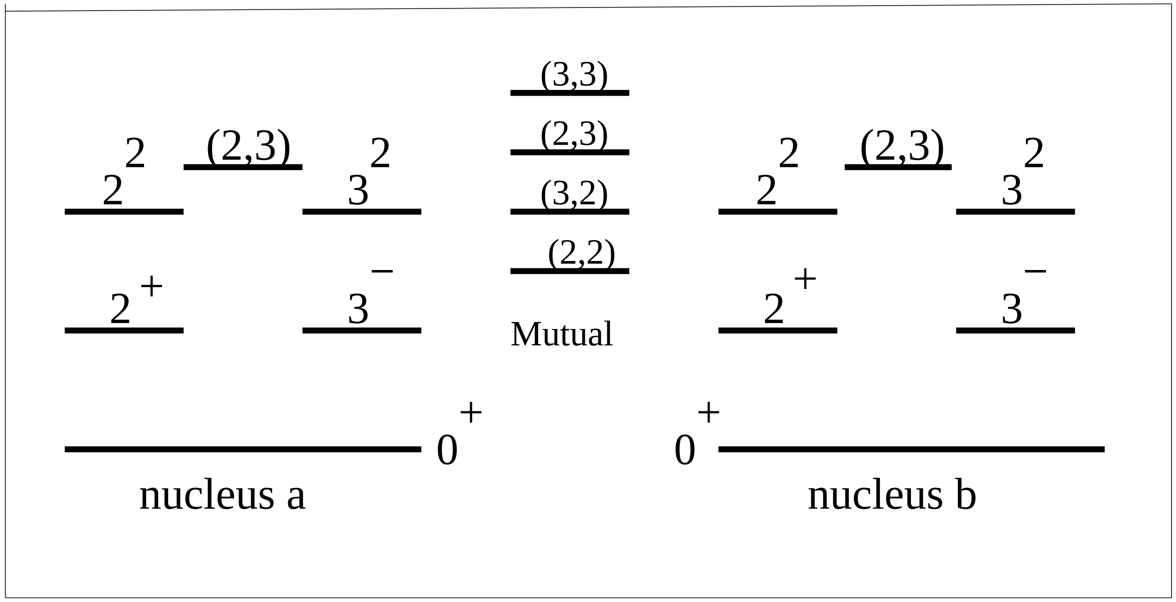

1 (GS) + 4 (1PH) + 4 (2PH) + 6 (Mutual) = 15 channels

(instead of the 138 channels of the full problem.)

This model works quite well for the fusion of not too heavy systems.

- It does not work for inelastic scattering at forward angles,
- in fusion reactions where transfer plays a role ($Q_{tr} > 0$),
- for heavy, soft or strongly deformed nuclei (multiple excitations),
- in heavy systems where deep inelastic reactions may play a role.

Standard coupled-channels calculations.

- Include nuclear couplings up to second order in the dynamic surface displacement $\delta s = R\sum \alpha_{\lambda\mu} Y^*_{\lambda\mu}(\hat{r})$,

$$U(r,\delta s) = U_N(r) - \frac{dU_N}{dr}\delta s + \frac{1}{2}\frac{d^2U_N}{dr^2}(\delta s^2 - \langle \delta s^2 \rangle),$$

  and Coulomb couplings up to first order in δs.

- Include one-phonon, two-phonon and mutual excitations of the low-lying 2^+ and 3^- states in projectile and target.

- Use scattering boundary conditions for large r,

$$\psi_{nI}(r) \rightarrow \delta_{nI,0I_0} e^{-ik_0 r} + R_{nI} e^{ik_n r}, \quad \text{for} \quad r \rightarrow \infty.$$

- Simulate fusion by ingoing-wave boundary conditions (IWBC),

$$\psi_n(r) \rightarrow T_n e^{-iq_n r}, \quad \text{for} \quad r \rightarrow R_{\text{pocket}},$$

which are imposed at the minimum of the pocket.

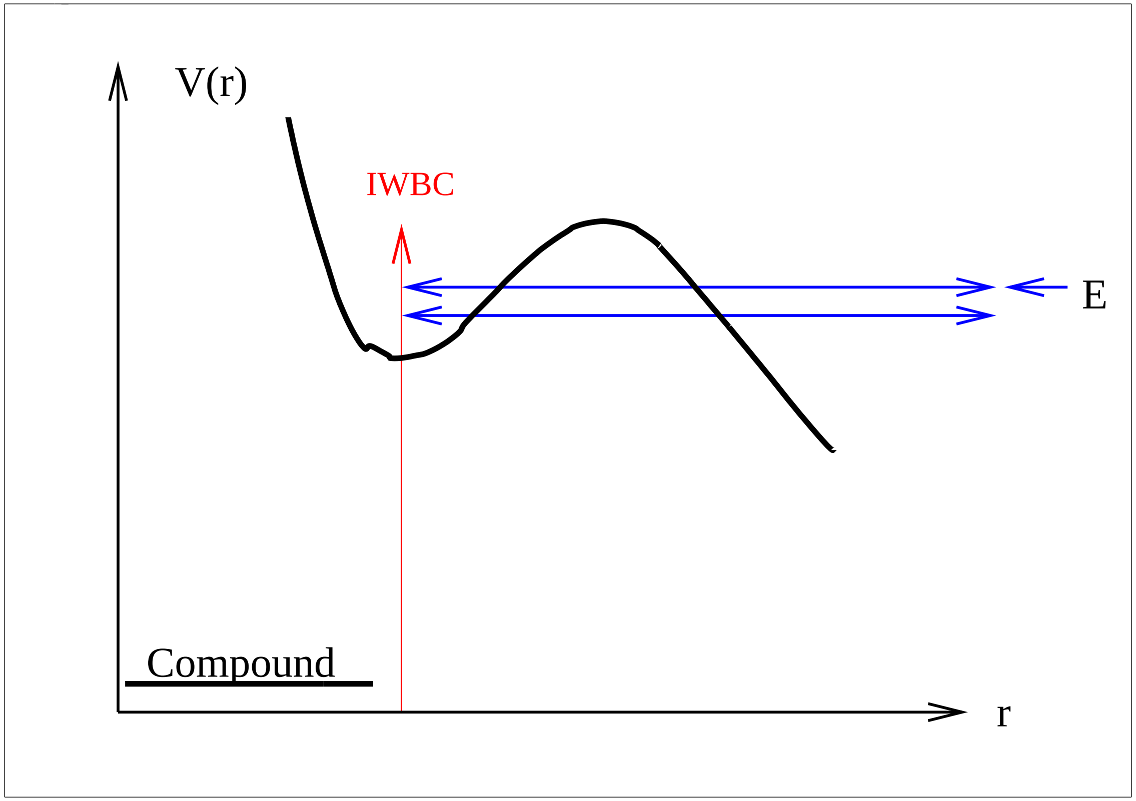

The IWBC are sometimes supplemented with a weak, short-ranged absorption.

Double folding potentials

$$U_N(\mathbf{r}) = \int d\mathbf{r}_1\, d\mathbf{r}_2\, \rho_a(\mathbf{r}_1)\, \rho_A(\mathbf{r}_2)\, v_{NN}(\mathbf{r}+\mathbf{r}_2-\mathbf{r}_1).$$

The effective M3Y interaction produces a very realistic Coulomb barrier, consistent with the proximity type Akyüz-Winther potential. However, the potential is way too deep for overlapping nuclei.

Supplement the M3Y interaction with a repulsive contact term,

$$v_{NN}^{\mathrm{rep}} = v_{\mathrm{rep}}\, \delta(\mathbf{r}+\mathbf{r}_2-\mathbf{r}_1).$$

Use a smaller diffuseness of the densities, $a_{\mathrm{rep}} \approx$ 0.3–0.4 fm, when calculating the repulsive potential.

Adjust the strength v_{rep} so that the total nuclear interaction for overlapping nuclei is consistent with the Equation of State,

$$U_N(r=0) = 2A_a[\epsilon(2\rho) - \epsilon(\rho)] \approx \frac{A_a}{9} K,$$

and a nuclear incompressibility of $K \approx$ 234 MeV.

Example: ^{64}Ni+^{64}Ni.

Mişicu and Esbensen, PRL 96, 112701 (2006).

The hindrance sets in below 89 MeV.

The hindrance is an entrance channel, and not a CN effect.

The shallow M3Y+Repulsion potential has been corrected for the effect of the nuclear incompressibility.

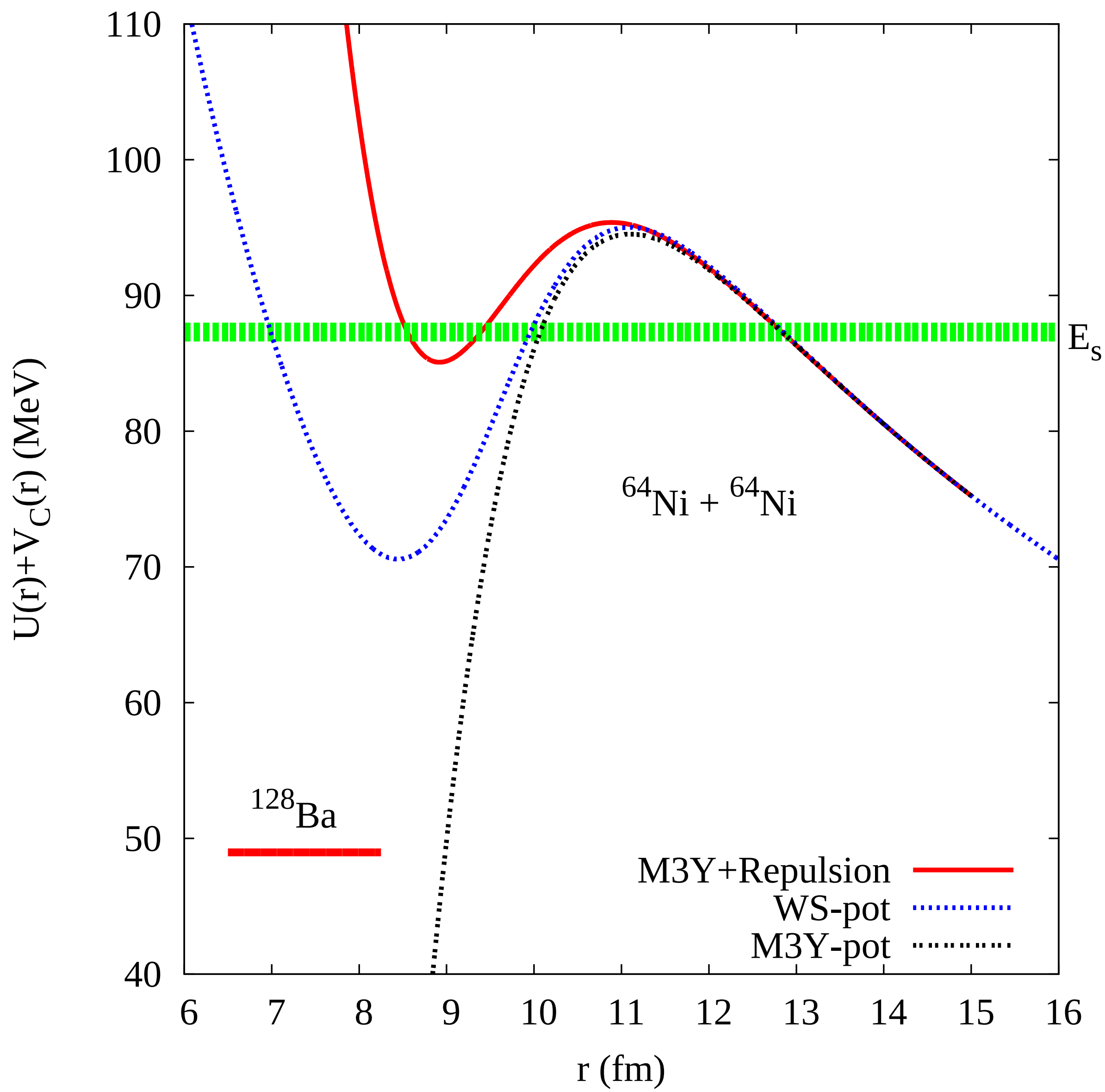

Applied to the ^{64}Ni+^{64}Ni fusion data

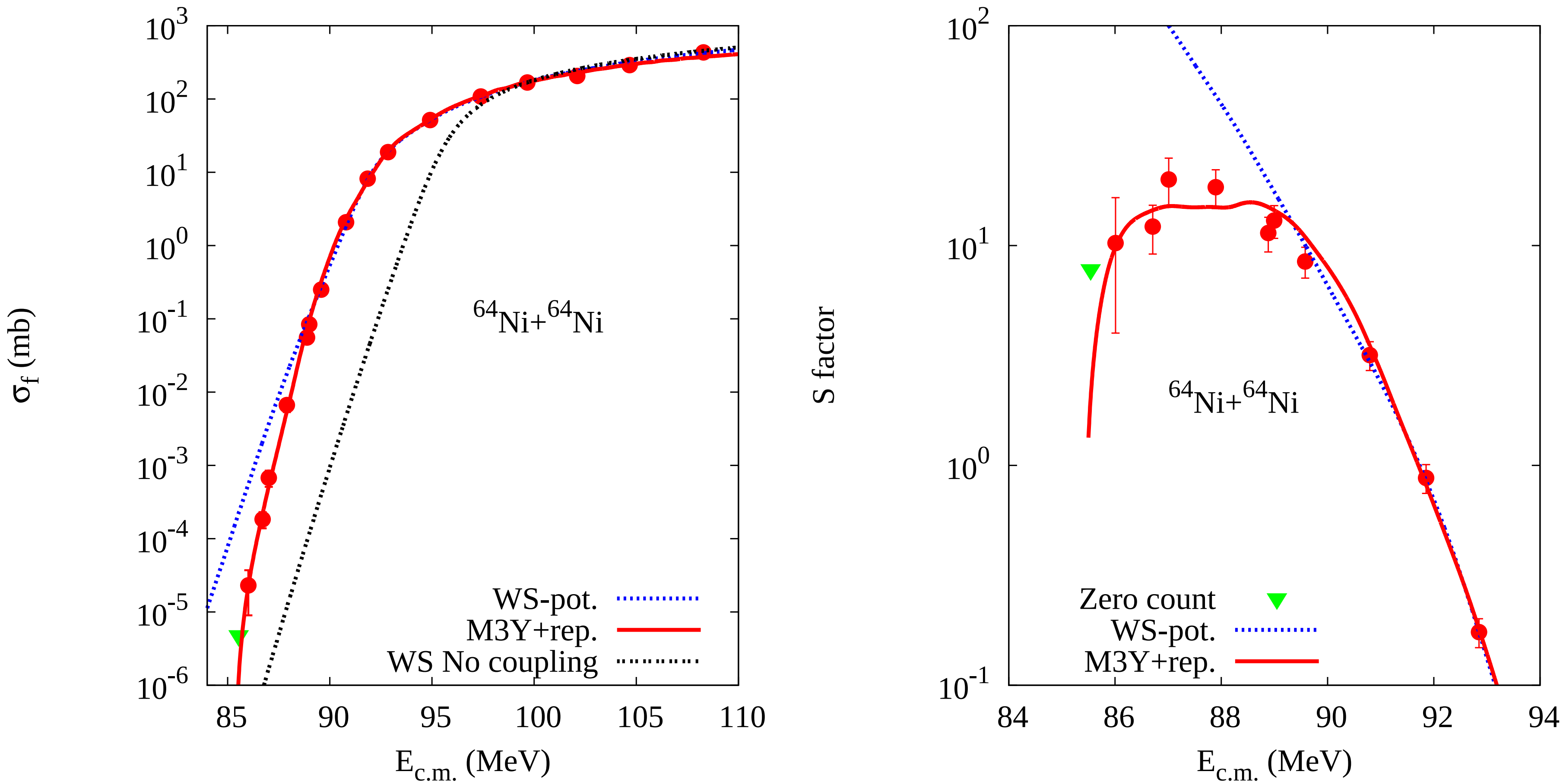

$$S - \text{factor} = E_{c.m.}\,\sigma_f\ \exp(2\pi[\eta - \eta_0]),\ \ \text{where}\ \ \eta = \frac{Z_1 Z_2 e^2}{\hbar v}.$$

The IWBC imply that $\sigma_f = 0$, for $E < V_{pocket} = 85.4$ MeV.

Average spin for fusion from γ-ray multiplicities.
Ackerman et al., NPA 609, 91 (1996).

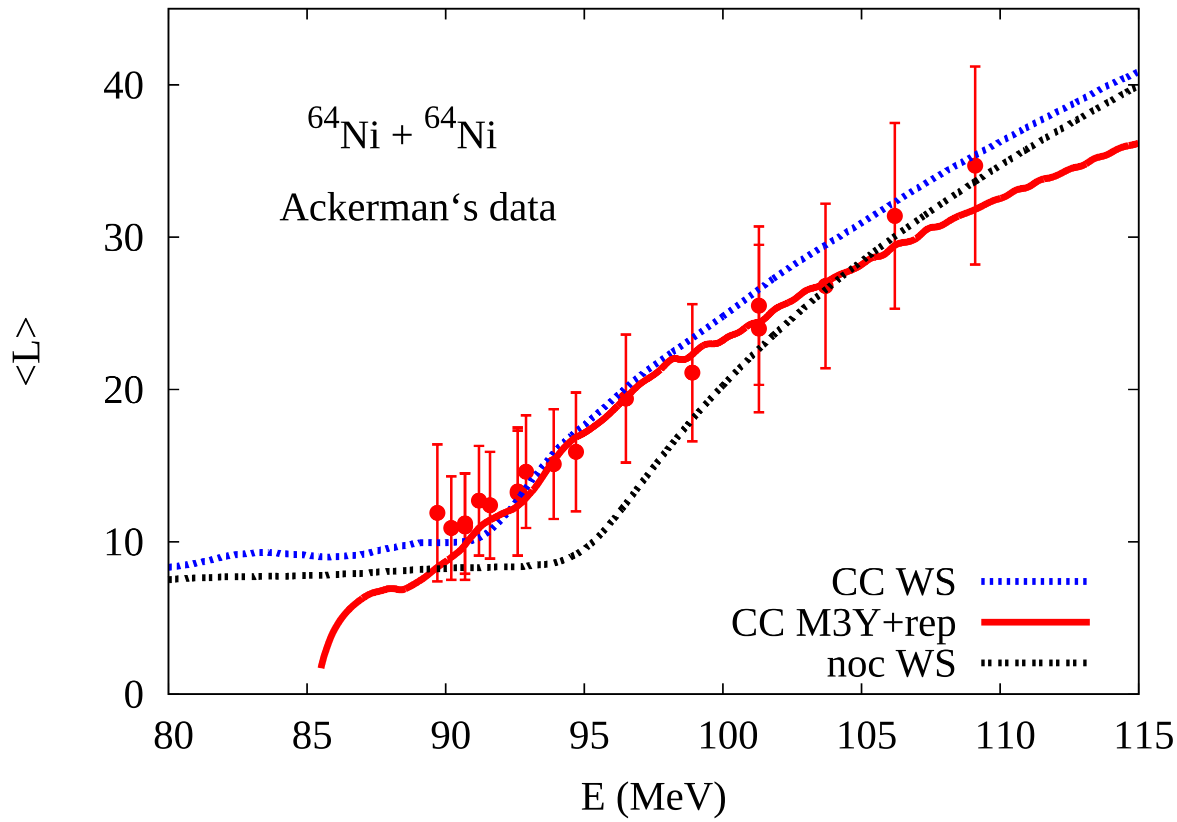

The WS potential predicts a constant average spin at low energy.

The (CC) M3Y+repulsion calculation predicts a vanishing spin at LE.

Mişicu and Esbensen, PRC 75, 034606 (2007).

Suppression at high energies

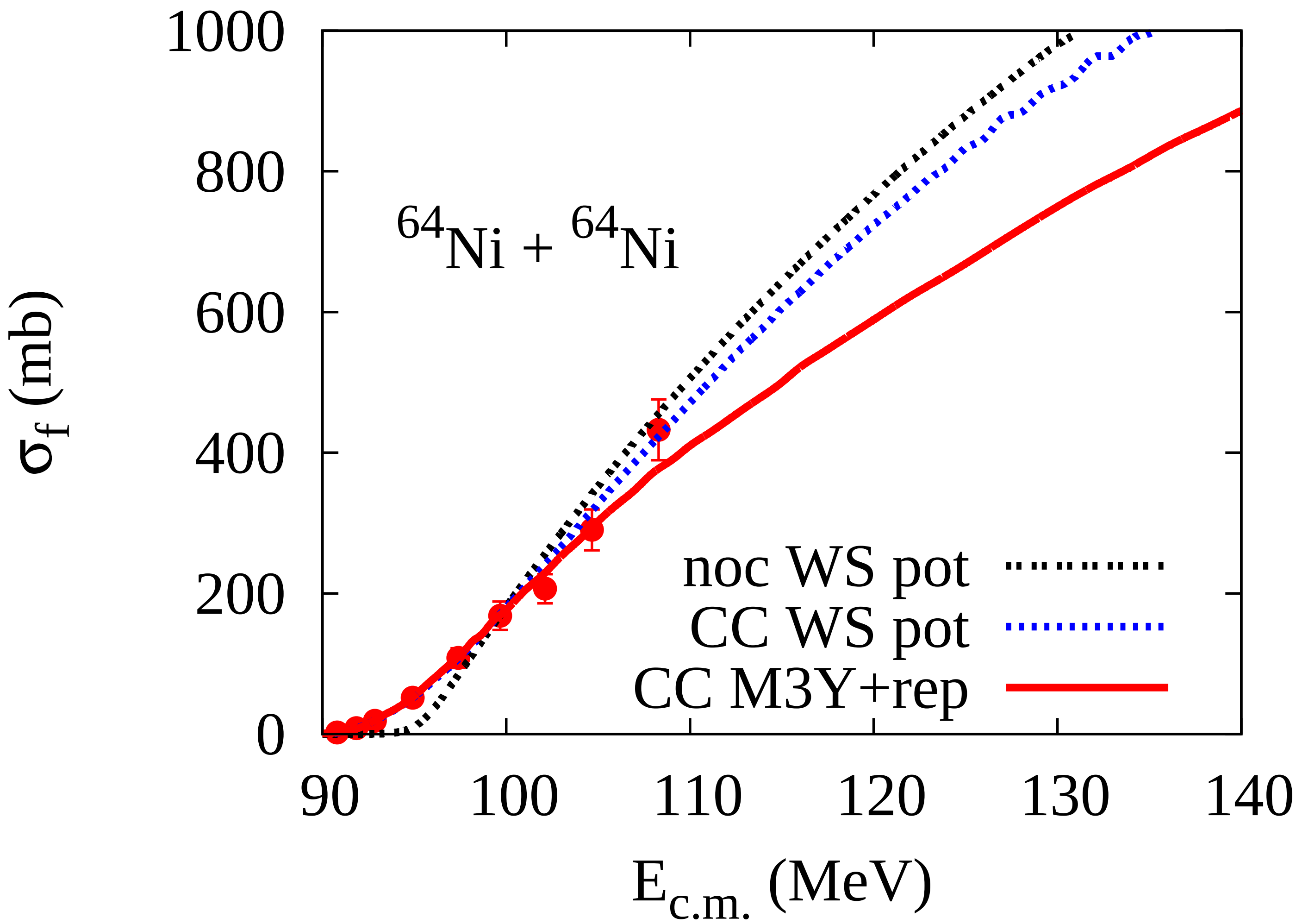

The M3Y+repulsion explains qualitatively the suppression that has been observed (for some systems) at high energies.

Signs of a fusion hindrance have been observed in many systems:
^{90}Zr+^{89}Y, +^{90,92}Zr, ^{28}Si+^{30}Si, ^{28}Si+^{64}Ni, ^{58}Ni+^{58}Ni, ^{64}Ni+^{64}Ni, ^{32}S+^{89}Y, ^{48}Ca+^{96}Zr, ^{60}Ni+^{89}Y, ^{64}Ni+^{100}Mo, ^{16}O+^{208}Pb.

Experimental work at Argonne, INFN Legnaro, and ANU Canberra.

Systematics by Jiang et al., Phys. Rev. C 73, 014613 (2006).

An example: ^{28}Si+^{64}Ni, Jiang et al., Phys. Lett. B 640, 18 (2006).

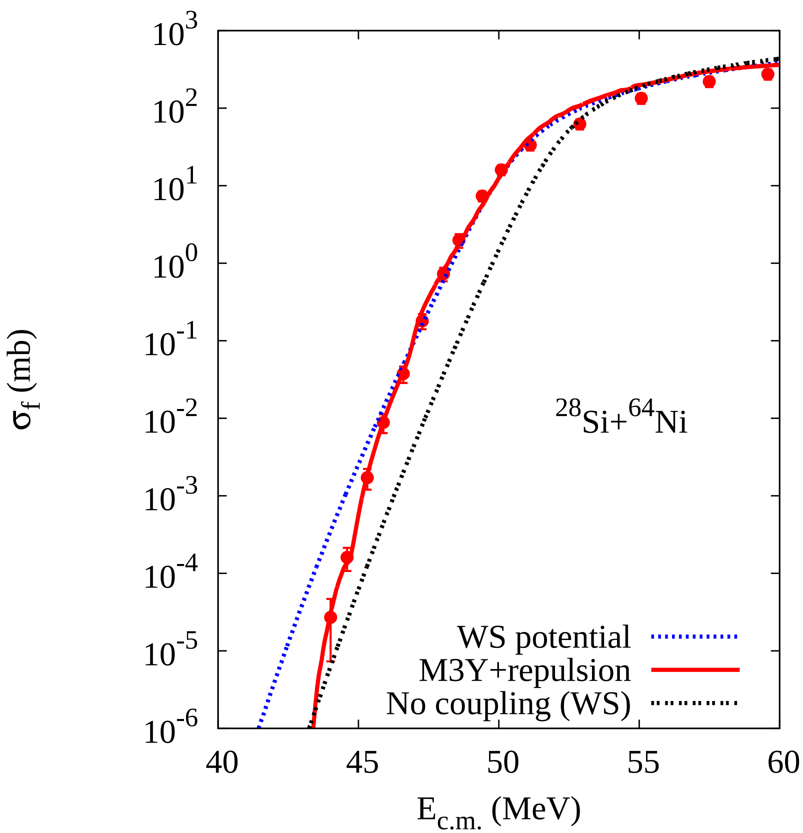

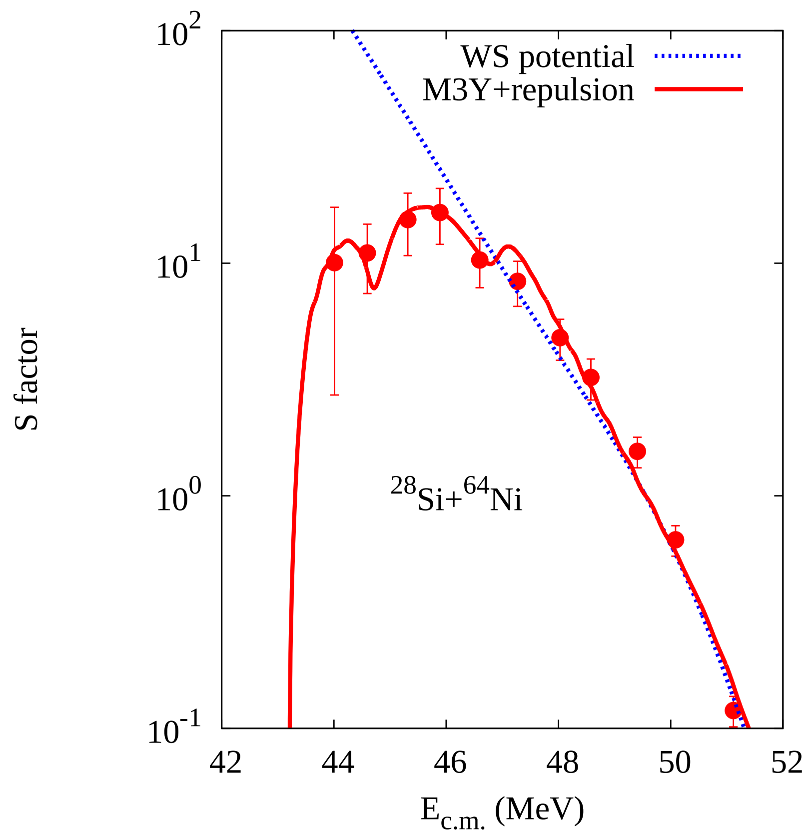

^{48}Ca+^{96}Zr fusion data, Stefanini et al., PRC 73, 034606 (2006).

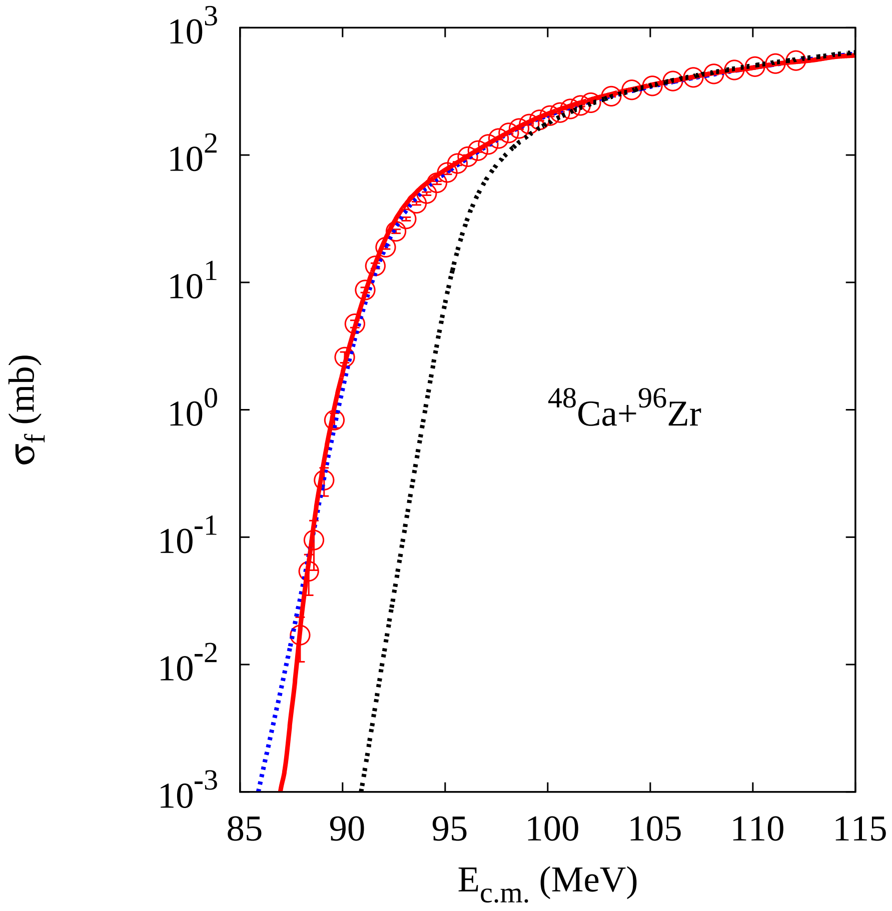

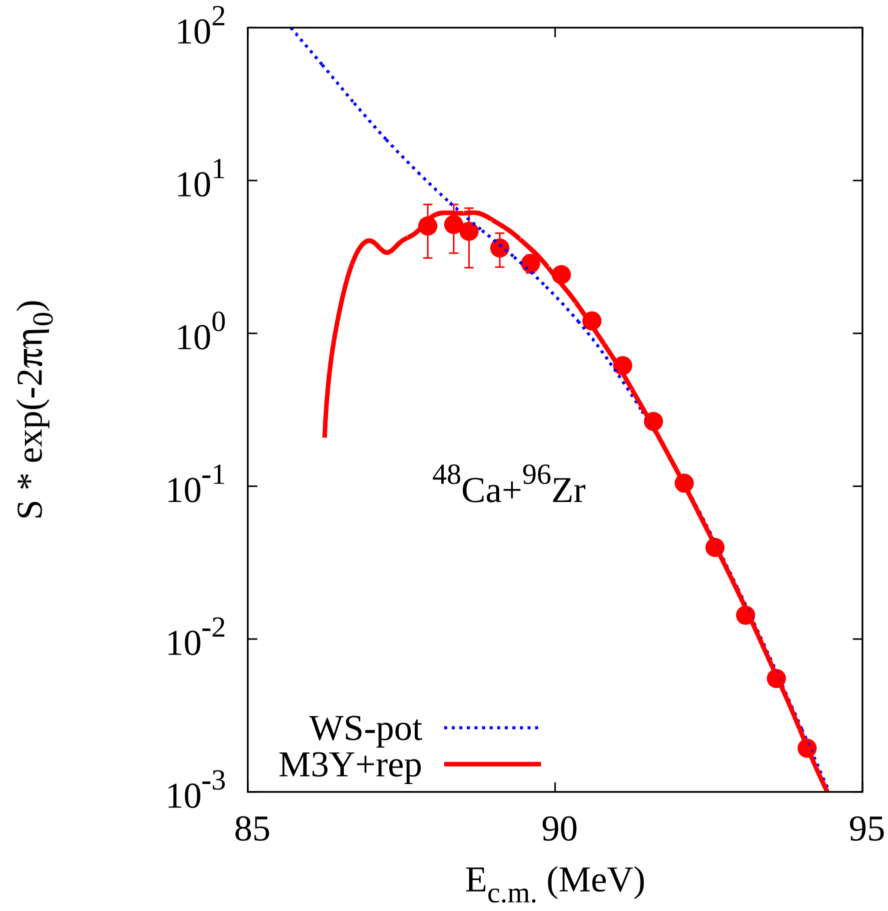

The M3Y+rep potential has a minimum pocket energy of V_{pocket} = 86.2 MeV. A maximum S factor barely reached.

PRC 79, 064619 (2009).

$^{16}O+^{208}Pb$ fusion, Morton et al., Phys. Rev. C 60, 044608 (1999).

New data (solid points), Dasgupta et al., PRL 99, 192701 (2007), confirm the fusion hindrance.

The WS potential is too deep and cannot explain the fusion hindrance.

A shallow pocket,
a thicker barrier,
and couplings to the
(^{16}O,^{17}O) transfer
explain the data much better,
HE&SM,PRC 76, 054609 (2007).

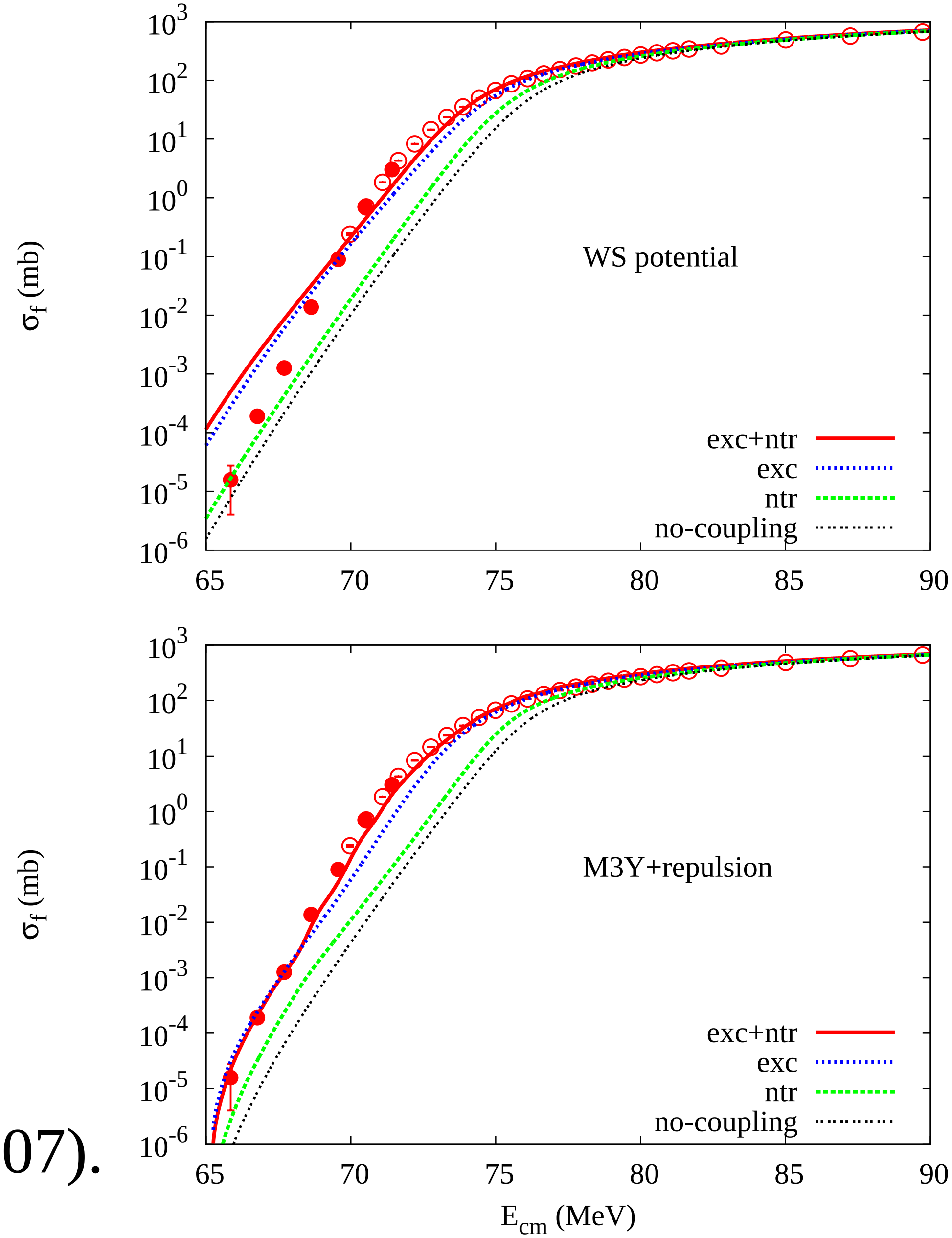

Entrance channel potential and S-factor

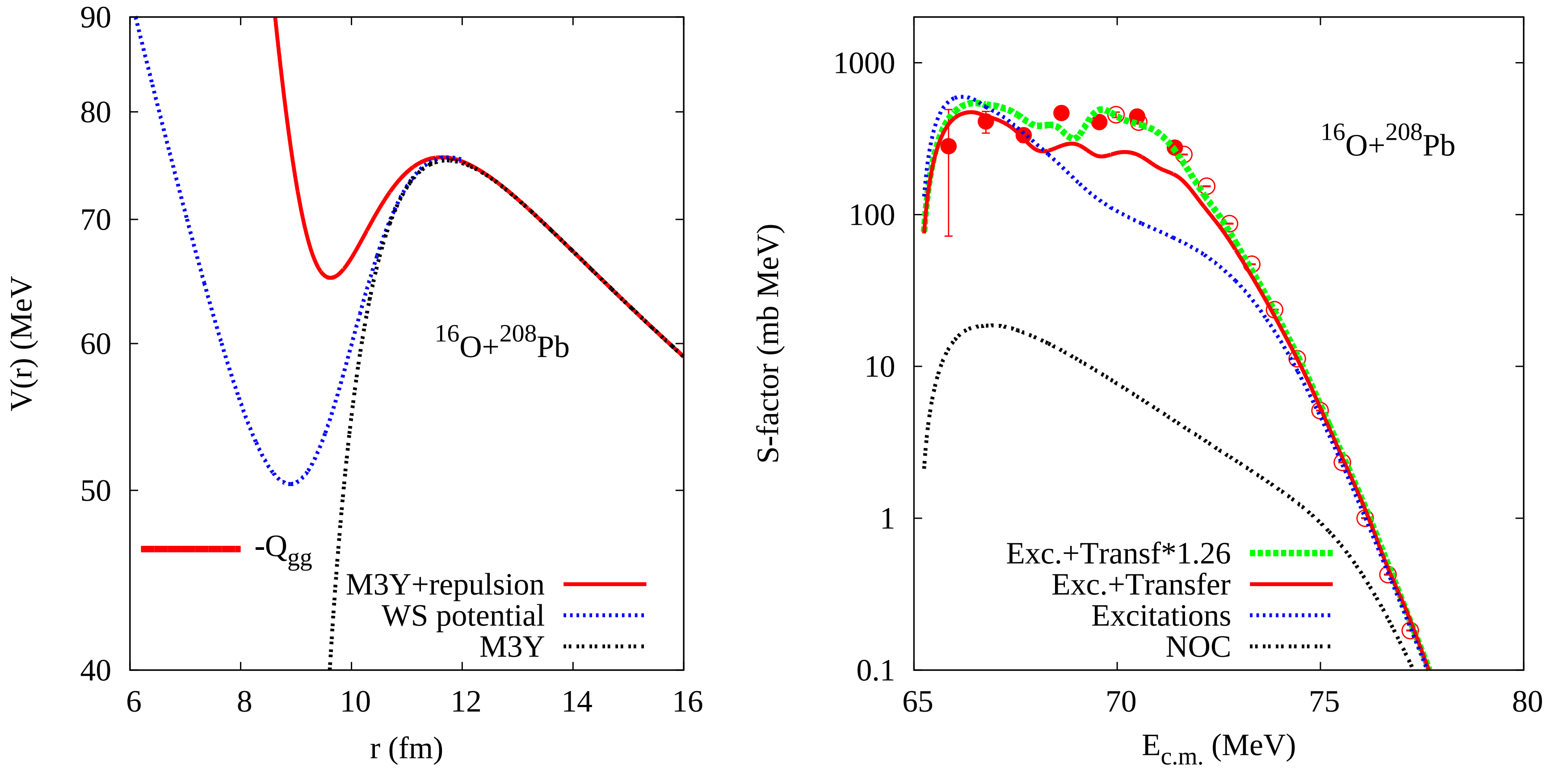

The M3Y+repulsion potential has a pocket at 65.1 MeV.

Green curve: one-neutron transfer strength was multiplied by 1.26.

This strength produces a realistic total reaction cross section.

Suppression of ^{16}O+^{208}Pb fusion far above the CB.

The high energy data are suppressed compared to calculations based on the WS potential.

The problem can be fixed by using a large diffuseness, Newton, PLB 586, 219 (2004).

Calculations based on the M3Y+repulsion potential and a weak, short-range absorption (SRAbs) reproduce the data.

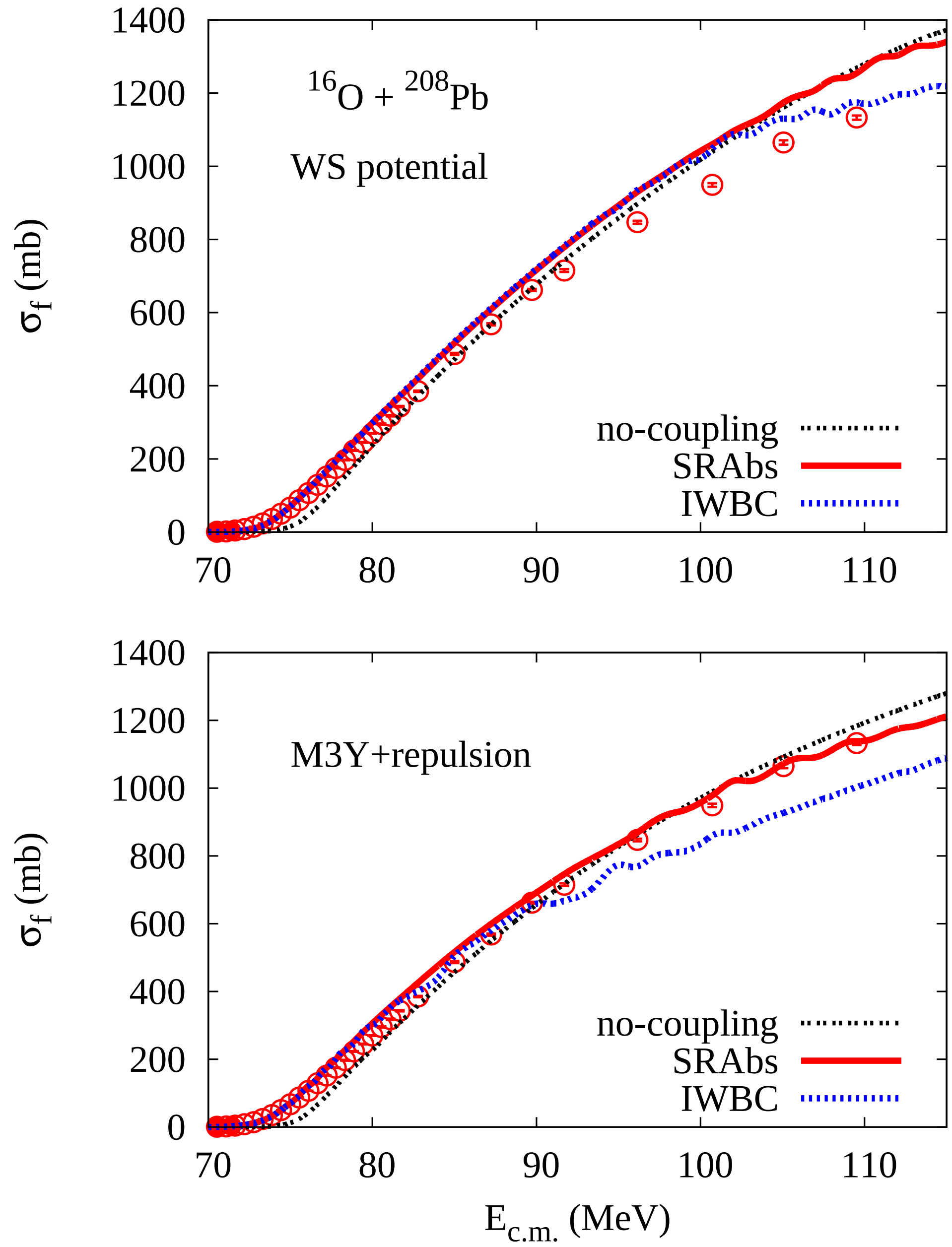

$^{16}O+^{16}O$ fusion data, Thomas et al., PRC 33, 1679 (1986).

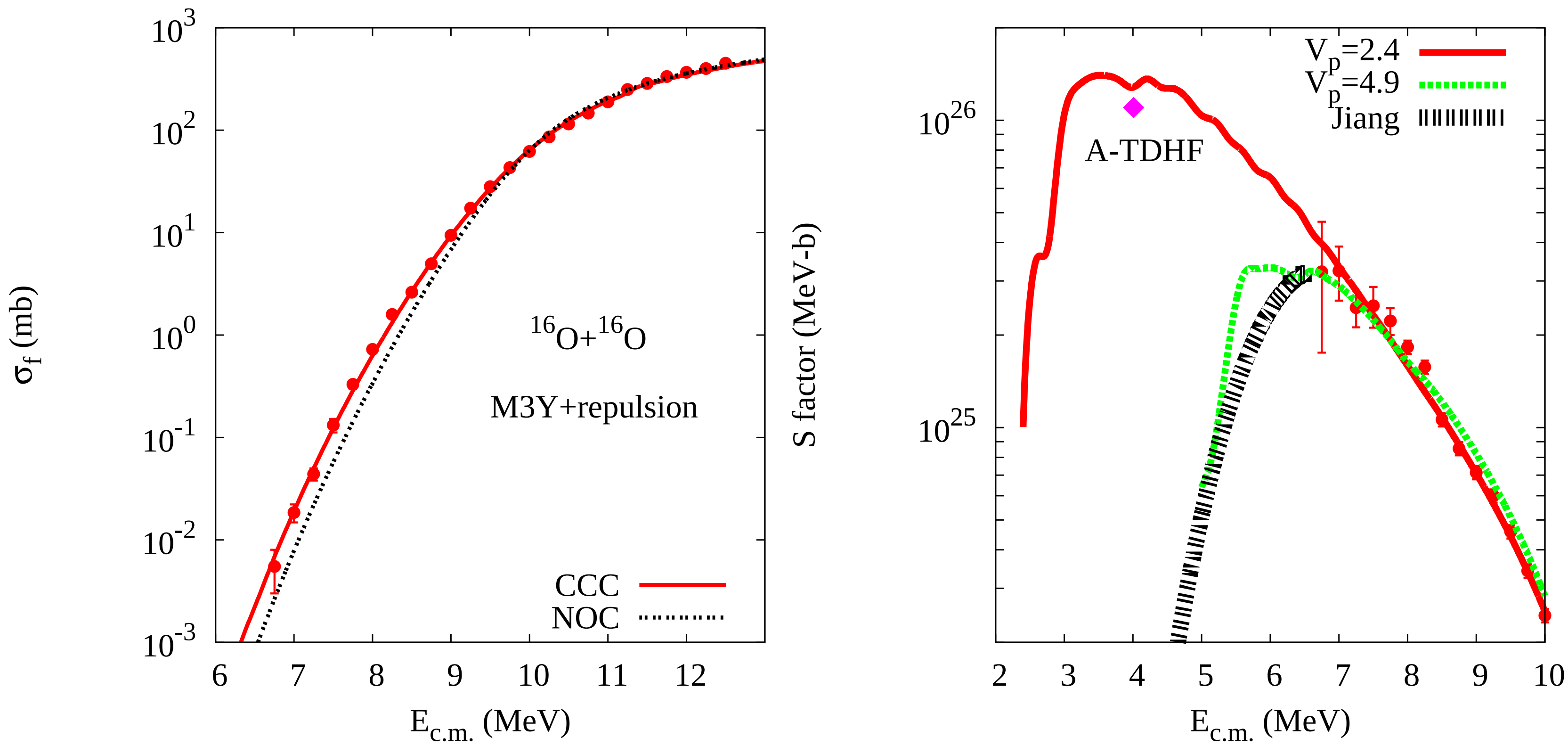

Red curve: best fit to all data points, HE, PRC 77, 054608 (2008).

Diamond: Adiabatic TDHF calc. by P.G.Reinhard et al.

Green: Best fit to 7 lowest points;

is consistent with Jiang’s extrapolation (black curve.)

Evidence for a shallow pocket in the fusion of $^{16}O+^{16}O$.

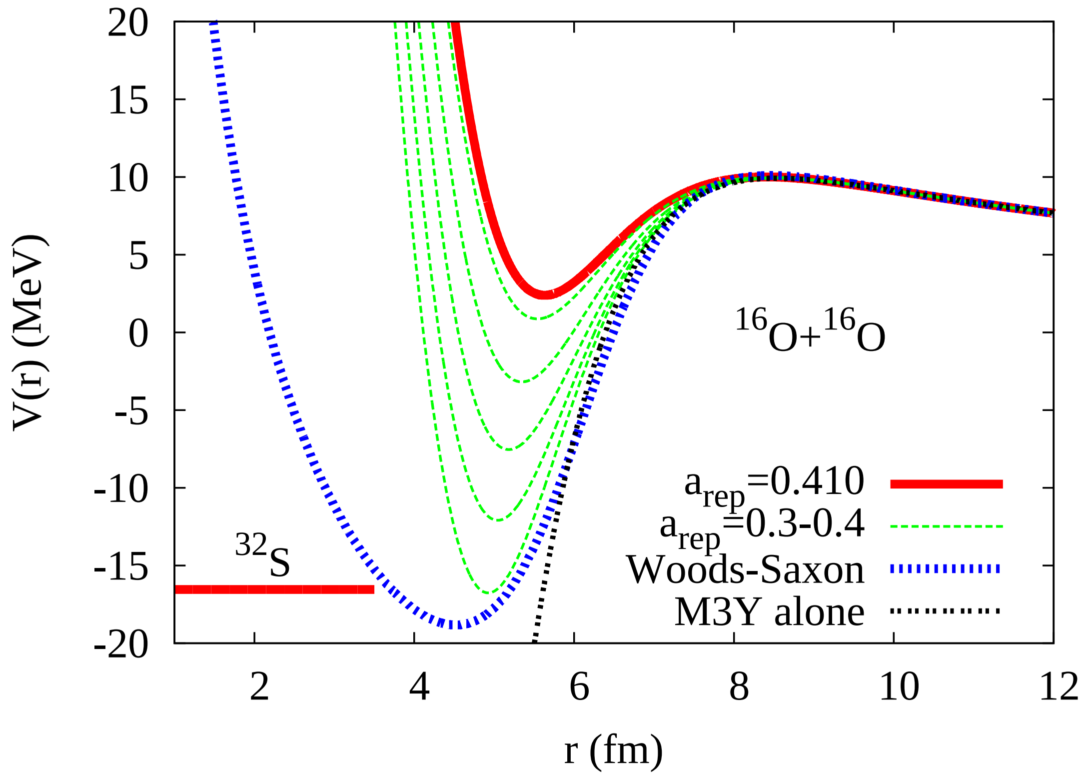

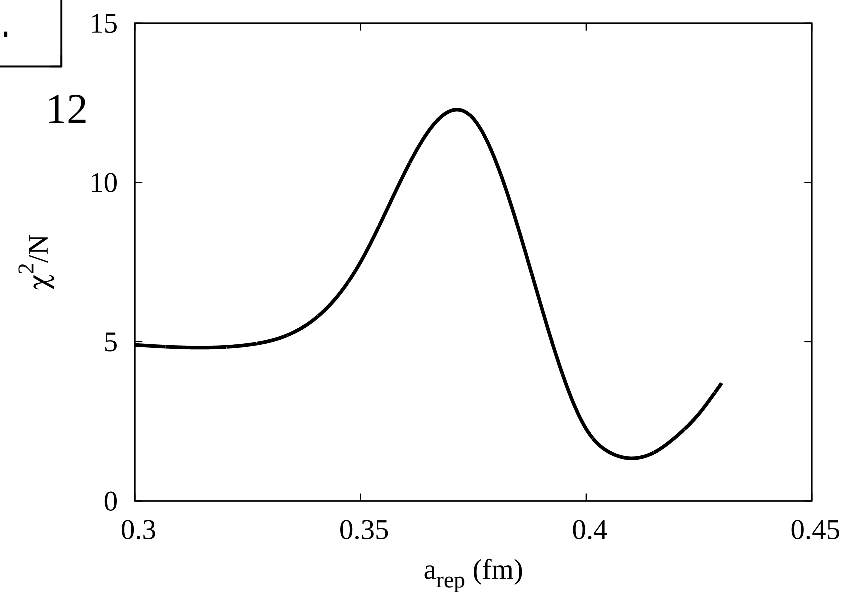

Vary $a_{\rm rep}$, adjust $v_{\rm rep}$ so K=234 MeV.
The best fit to Thomas's data is
obtained for $a_{\rm rep}$ = 0.41 fm...

$^{16}O+^{16}O$ high energy fusion.

Diamonds data by Tserruya et al. (1978).

Kolata et al. (1977) saw similar structures.

Are also been seen in $^{12}C+^{12}C$ fusion.

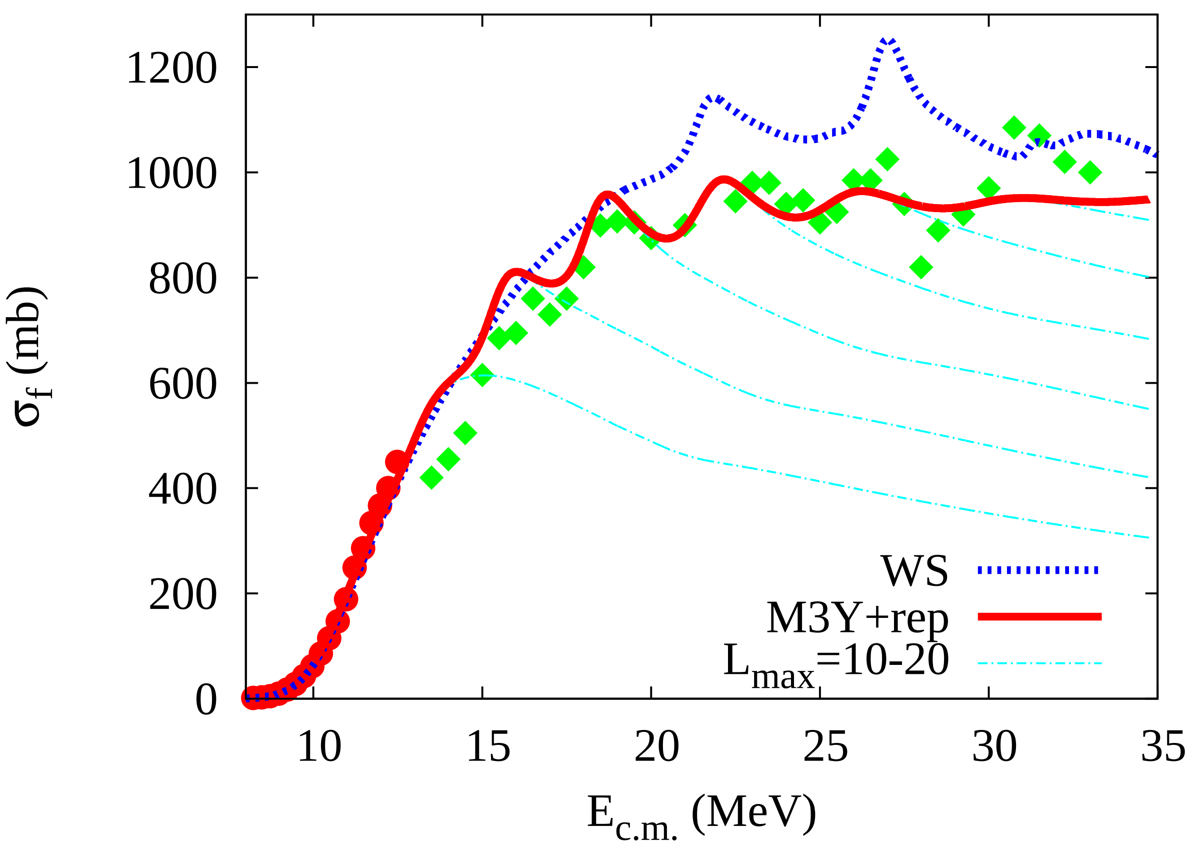

Blue dashed curve: based on conventional Woods-Saxon well.

Red curve: the M3Y+rep calculation that fits the Thomas data.

The high energy data prefer a shallow pocket. Consistent with elastic scattering analysis by Gobbi et al. PRC 7, 30 (1973).

Conclusion

- The hindrance of fusion far below the Coulomb barrier is a general phenomenon, which has been observed in many heavy-ion systems.
- It is explained by (a posteriori) coupled-channels calculations that are based on IWBC and a shallow potential in the entrance channel.
- A shallow potential also helps resolve the problem of a suppression of high energy fusion data and explains the structures observed in the high energy $^{16}O+^{16}O$ fusion and scattering data.
- A short-range imaginary potential is often needed at high energies to simulate the effect of the many channels that open up.
- Going beyond the Rotating Frame Approximation would be a computational challenge and require a large number of channels.

Open questions

- Expand experimental and theoretical studies to lighter systems. WILL THE HINDRANCE PERSIST, and how will it affect the extrapolation to astrophysical reaction rates?
  (Gasques et al., PRC 76, 035802, 2007).
- What is the relation to molecular resonances (Bromley et al.)?
- What is the relation to TDHF calculations (Oberacker and Umar)?
- How does the hindrance affect the production of heavy elements?
- How to model the dynamics all the way to the compound nucleus?
  (Ichikawa et al., PRC 75, 057603 (2007)).

Future directions

- Study more reactions of interest to astrophysics.
- Study the competition between breakup, complete and incomplete fusion of weakly bound nuclei.
- Apply CDCC calculations to deal with states in the continuum.
- A good starting point is ^{9}Be. It has several advantages:
  it is weakly bound, $Q(\alpha + \alpha + n)$ = - 1.574 MeV, with only one (borromean) bound state. It is stable (strong beams).
  Many experiments have already been performed.

^{9}Be is strongly deformed, Q_0 = 26.5 (15) fm^2.

$$\rho(r,\theta') = C\frac{1+\cosh(R(\theta')/a)}{\cosh(r/a)+\cosh(R(\theta')/a)}, \quad R(\theta') = R_0(1+\beta_2 Y_{20}(\theta')).$$

θ' is the angle between **r** and the symmetry axis. Calibrate the density to give the correct RMS charge radius and quadrupole moment Q_0.

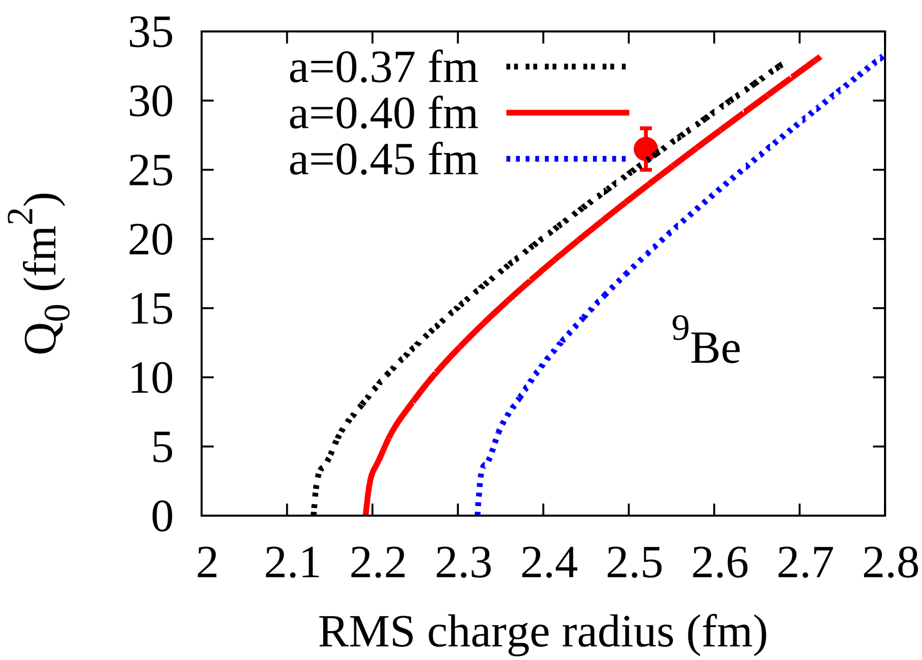

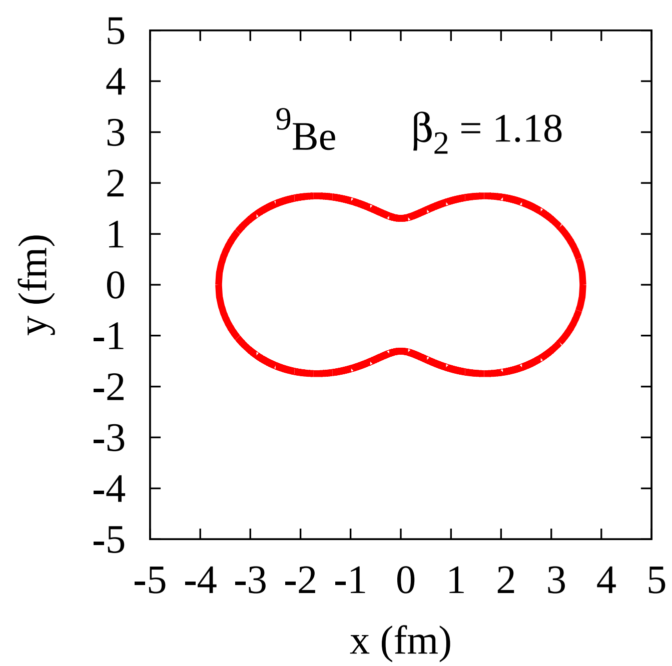

This is achieved for R_0=2.08, a=0.375 fm, and β_2 = 1.18.

Coupled Eqs. for excitations of the Ground State rotational band of ^{9}Be.

Spins: I^π = $3/2^-$, $5/2^-$ and $7/2^-$, exc. energies 0.0, 2.43 and 6.38 MeV.

The decay of the $7/2^-$ state, $\Gamma(7/2^-)$ = 1.21 MeV, is included as an absorption. It may lead to incomplete fusion (ICF).

Coupled equations:

$$\Big[\frac{\hbar^2}{2\mu}\Big(-\frac{d^2}{dr^2}+\frac{l(l+1)}{r^2}\Big)+U_0(r)+\mathbf{E_I}-\mathbf{i\Gamma_I/2}-E_{cm}\Big]\psi_{IM}(r)$$

$$=-\sum_{\lambda>0}\sum_{I'}\langle KIM|P_\lambda(\cos(\theta'))|KI'M\rangle\, U_\lambda(r)\,\psi_{I'M}(r).$$

Esbensen, PRC 81, 034606 (2010).

K=3/2 Ground State channel potentials and the complete fusion (CF) of ^{9}Be and ^{144}Sm.

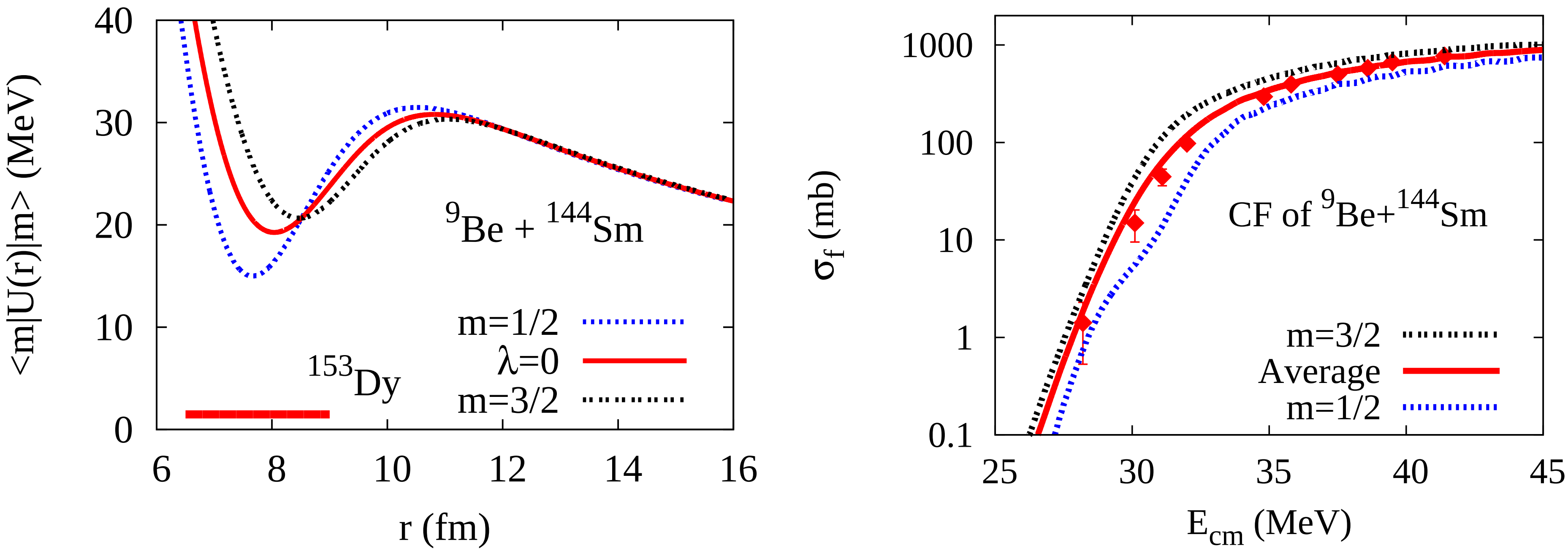

Fusion through the tip (m=3/2) dominates at low energy.

Fusion through the belly (m=1/2) is hindered at low energy.

Complete (CF) and incomplete (ICF) fusion

of ^{9}Be and ^{144}Sm, Gomes et al., PRC 73, 064606 (2006).

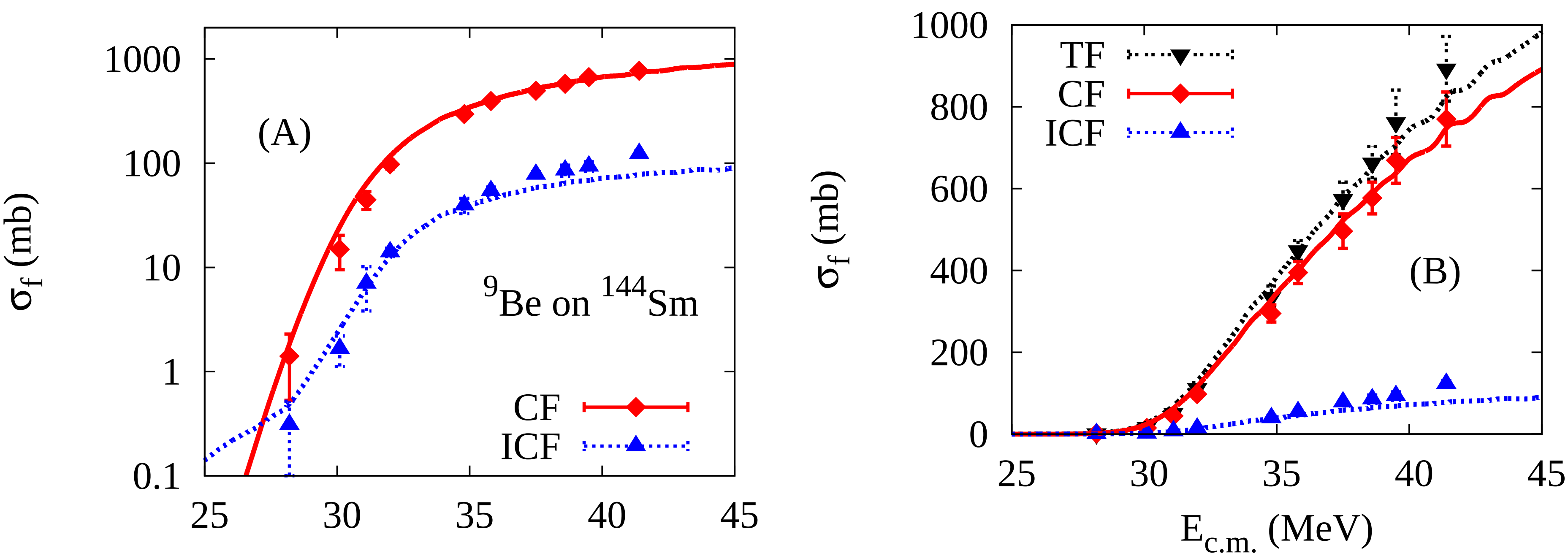

CF reproduced by IWBC. ICF reproduced by the decay.

Complete (CF) and incomplete (ICF) fusion

of ^{9}Be and ^{208}Pb, Dasgupta et al., PRC 73, 024606 (2004).

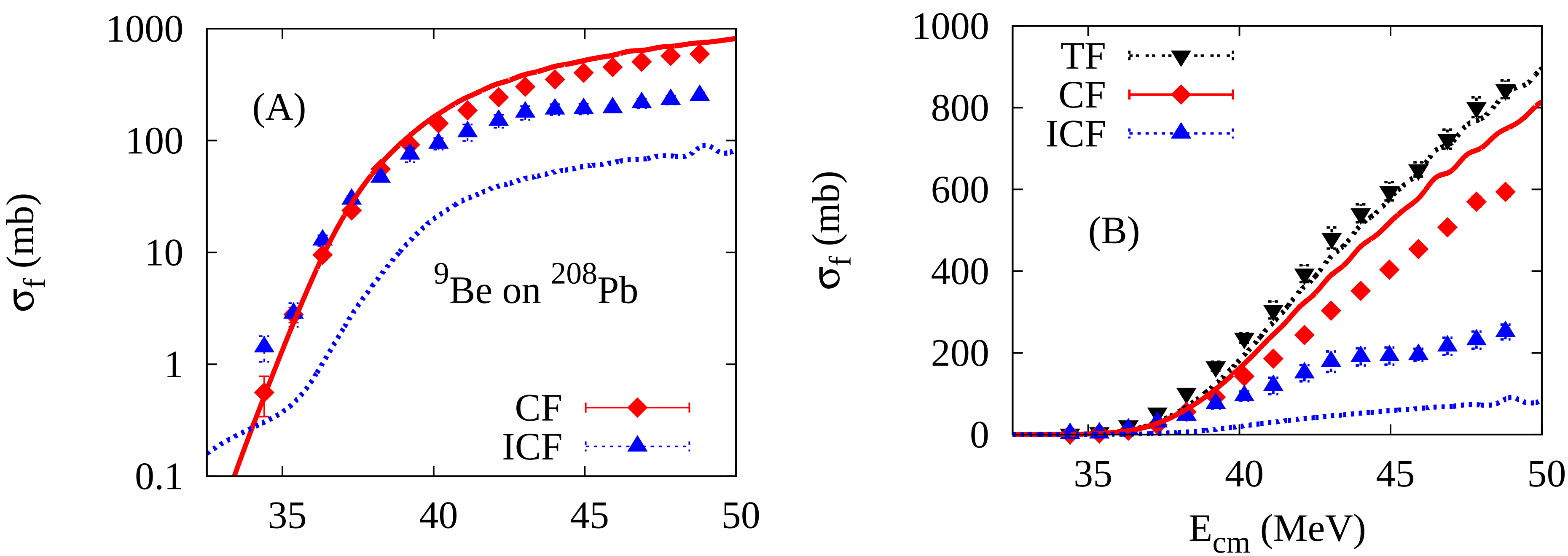

CF data are suppressed by 20%. The decay explains only 1/3 of ICF.

Include a weak absorption in addition to decay,

$$W(r) = \frac{-i\,0.35\ \mathrm{MeV}}{1 + \exp((r - 11.5)/0.4)}.$$

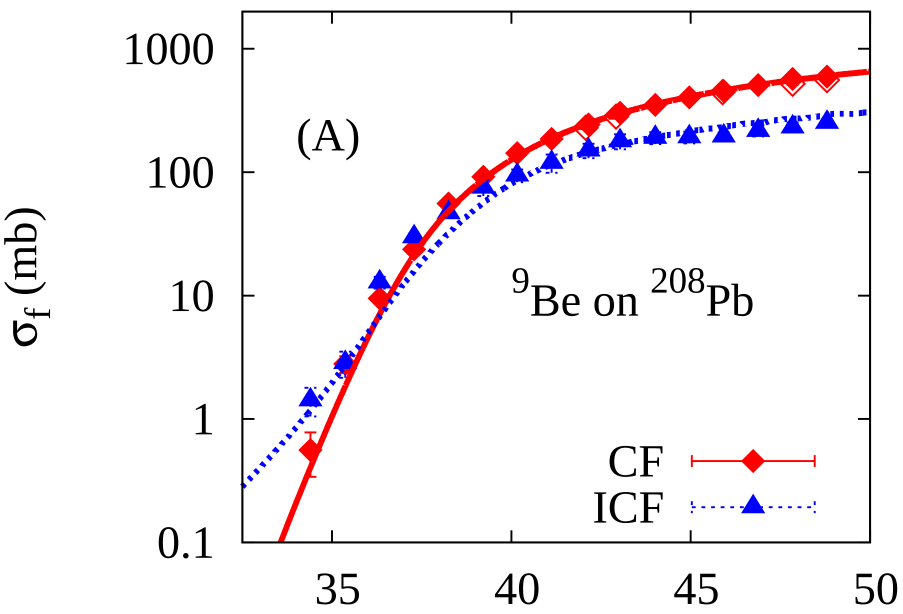

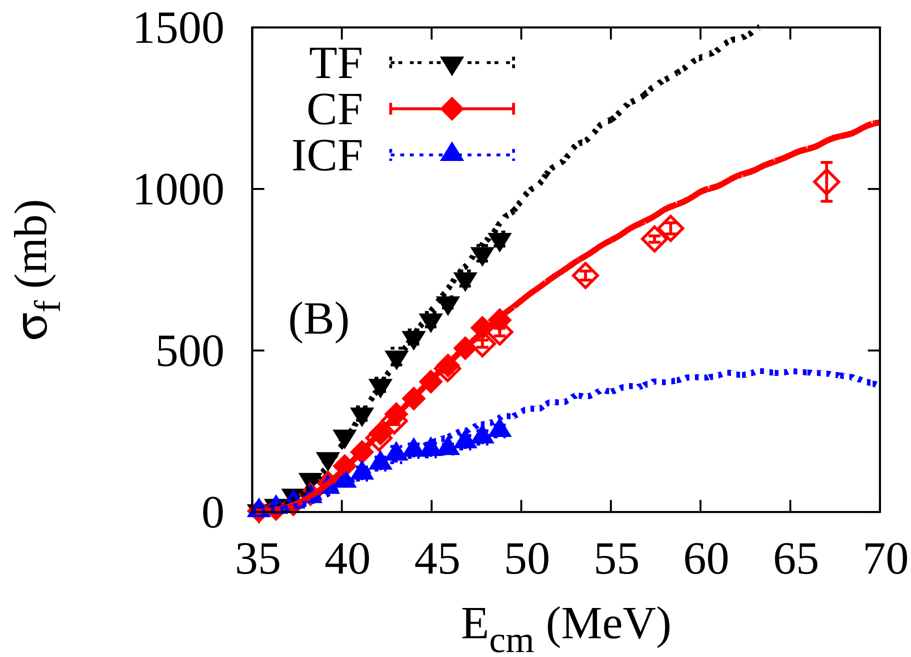

One-neutron transfer is the most likely reaction mechanism
responsible for the breakup and ICF of ^{9}Be,
Rafiei et al., incl. Diaz-Torres, PRC 81, 024601 (20101).